Lineament analysis in the outcropping rocks of the Ouaouizaght syncline, Central High Atlas

Análisis de lineamientos en las rocas que afloran en el sinclinal de Ouaouizaght, Alto Atlas Central

Hassane El makrini[1], Moussaid Bennacer[2], Hmidou El-Ouardi[1], Mahamat Ibrahim Ivanof Régis[1] and Ould Mohamed Vall Mohamed[1]

[1] CartoTec group, UMI, Faculty of Sciences, PB. 11201 Zitoune, Meknes, Morocco. h.elmakrini@gmail.com; ibrahim2brazza@yahoo.fr; h.elouardi@fs-umi.ac.ma, medmedvall87@gmail.com

[2] Laboratoire de «BGIM», Ecole Normale Supérieure, Université Hassan II, Ghandi Casablanca BP: 500 69, Morocco. bnmous@hotmail.fr

ABSTRACT

*In this work, we perform a lineament analysis of the Ouaouizaght syncline area (Central High Atlas, Morocco) in terms of their structural and tectonic significance. The methodology consists of satellite image (Lansat 8 OLI) processing by means of principal component analysis (PCA). The maximum of lineament orientation in the study area shows a NE-SW direction and two relative maxima oriented N0 and N90. The higher density areas of lineaments are located along the four borders of the Ouaouizaght syncline probably highlighting the importance of major faults characterized by diapiric processes (*e.g.*, movement of salt towards the anticline cores delimiting the Ouaouizaght syncline) during the extensional stage and importance of these previous discontinuities in the subsequent tectonic inversion.*

Key-words: *Ouaouizaght syncline, lineament analysis, satellite image analysis.*

RESUMEN

*En este trabajo realizamos un análisis de lineamientos en el área del sinclinal de Ouaouizaght (Atlas Alto Central, Marruecos) para entender su significado estructural y tectónico. La metodología consiste en el procesamiento de la imagen de satélite Lansat 8 OLI por medio de un análisis de componentes principales. La orientación principal de los lineamientos obtenidos que se deduce en el área de estudio es NE-SO y además se observan dos máximos relativos orientados N0 y N90. Las áreas que presentan una mayor densidad de lineamientos se localizan a lo largo de los cuatros márgenes del sinclinal de Ouaouizaght. Esto probablemente refleja la importancia de las fallas principales caracterizadas por procesos diapíricos (*e.g.*, movimiento de sal hacia los núcleos de los anticlinales que bordean el sinclinal de Ouaouizaght) durante la etapa extensional y la importancia de estas discontinuidades previas en la posterior inversión tectónica.*

Palabras clave: *sinclinal de Ouaouizaght, análisis de lineamientos, análisis de imagen satélite.*

Geogaceta, 66 (2019), 119-122
ISSN (versión impresa): 0213683X
ISSN (Internet): 2173-6545

Recepción: 1 de febrero de 2019
Revisión: 25 de abril de 2019
Aceptación: 24 de mayo de 2019

Introduction

Lineaments are natural and linear terrestrial surface features interpreted directly from satellite images and geophysical maps, called fracture traces (O'leary *et al.,* 1976; Moore and Waltz, 1983).

Mapping and lineament analysis from remote sensing data is an important approach for regional structural and tectonic studies (Solomon and Ghebreab, 2006).

The aim of this work is to analyse the lineaments of the Ouaouizaght syncline in terms of their structural and tectonic significance, processing image satellite data and the geological map.

Geological setting

The study area is part of the northern edge of the Moroccan Central High Atlas. The structure of the Central High Atlas is characterized by the occurrence of several anticlines oriented NE-SW (longitudinal ridges) and NW-SE (transverse ridges) delimiting synclines formed by Jurassic-Cretaceous deposits (Laville, 1985). The Ouaouizaght syncline constitutes one of these NE-SW synclines (Fig. 1) with a slight curvature in its western part. It is an asymmetrical syncline whose NW limb presents a more complete stratigraphic succession than that of the SE limb, which becomes thinner toward the Lower Jurassic ridge of Jbel el Abbadine (Haddoumi *et al.*, 2010). The anticlinal ridges, developed from the basinal stage, have played a major role controlling the Jurassic-Cretaceous sedimentation in the High Atlas area and its structure during the subsequent tectonic inversion. Several authors point to a diapiric origin for these structures (Michard *et al.*, 2011; Saura *et al.*, 2014; Moragas *et al.*, 2017; Torres-López *et al.*, 2018). The study area comprises the Ouaouizaght syncline and the area delimited between the Aghbala-Afourer fault zone in the north and the Jbel Abbadine anticline in the south (see Fig. 1).

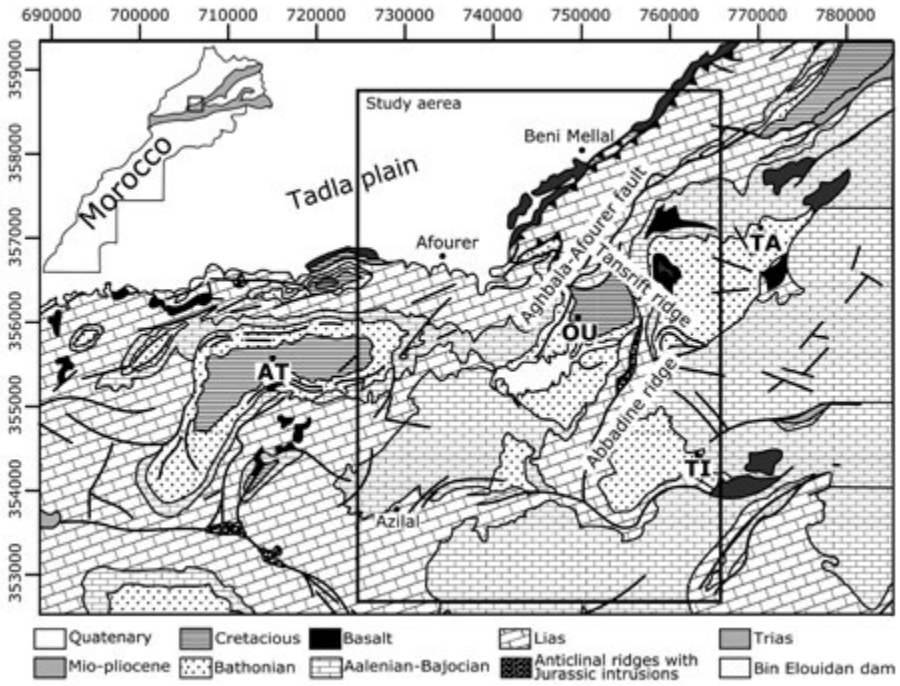

Fig. 1.- Geological map of the Ouaouizaght syncline and surroundings (modified from Monbaron, 1985). AT: Aït Attab; OU: Ouaouizeght; TA: Tagelft; TI: Tilouguit.

Fig 1.- Mapa geológico del sinclinal de Ouaouizaght y alrededores (modificado de Monbaron, 1985). AT: Aït Attab; OU: Ouaouizeght; TA: Tagelft; TI: Tilouguit.

The Aghbala-Afourer fault zone, in the north, permits the limestones and dolomites of the Lower Jurassic platform series to overlap and thrust over the Cretaceous series of the northern part of the syncline. To the south, the Ouaouizaght syncline is bounded by the diapiric Jbel Abbadine anticline with its southwestern extension, which separates the former from the Tilouguit basin to the south and Aït Attab to the west. In addition to these two atlasic structures, the Ouaouizaght basin is separated to the east from the Taguelft basin by the NW-SE trending diapiric ridge of Tansrift.

Methodology

Processing:

The methodology consists of satellite image processing by means of principal component analysis (PCA).

We used a Landsat 8 OLI satellite image, already corrected geometrically, consisting of eleven bands, from which the first seven were analyzed in this work. This image has undergone atmospheric preprocessing based essentially on dark objects substraction in order to have reflectance at the soil level, to obtain a maximum of information on different spectra (Moore and Waltz, 1983; Van der Werff and van der Meer, 2016).

Principal Components Analysis

Principal components analysis (PCA) allowed us to compress all the information contained in the different bands with one, two or three components.

This operation shows a considerable spectral enrichment, providing improvement and precision of the geological discontinuities. It also shows contrasts between different outcrops (Fig. 2), which facilitated the determination of the lineaments. The PCA synthesized 96.15% of the information contained in the original multispectral image. It shows a clear correlation between some bands (Table I).

The directional filtering of the resulting image of the PCA permits to highlight and classify the contrasts following each direction.

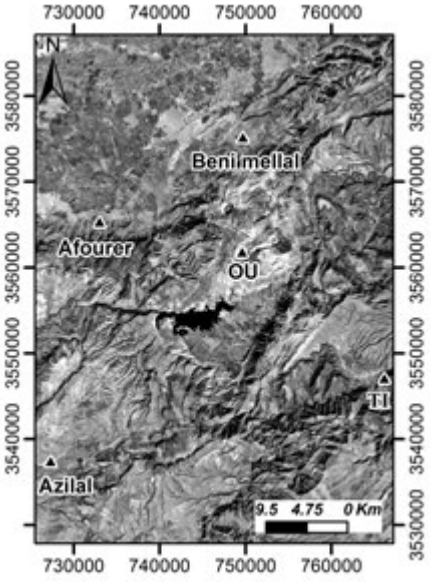

Fig. 2.- First component principal (CP1) issue the PCA.

Fig. 2.- Primer componente principal (CP1) emite el PCA.

Corre-lation	PC1	PC2	PC3	PC4	PC5	PC6	PC7
Band 1	-0.375	-0.378	-0.383	-0.381	-0.375	-0.378	-0.375
Band 2	-0.539	0.449	0.172	-0.129	-0.080	-0.458	-0.495
Band 3	-0.020	0.102	0.233	0.337	-0.860	-0.078	0.276
Band 4	0.413	0.127	-0.323	-0.642	-0.246	0.322	0.363
Band 5	-0.346	0.150	0.588	-0.401	-0.125	0.467	-0.343
Band 6	-0.203	0.021	0.412	-0.387	0.189	-0.565	0.533
Band 7	-0.487	0.778	-0.387	0.038	0.036	-0.037	0.060

Table I. Correlation matrix of landsat TM bands.

Tabla I.- Matriz de correlación de bandas Landsat TM.

Directional filtering

In geology, we are interested in lineaments of natural origin, which most often correspond to topographic ridges, contacts between different lithologies, fracture lines and/or faults (Nicolini, 1980; Scanvic, 1983).

The application of the 7x7 sobel filter in the four directions N-S, E-W, NW-SE and NE-SW (Table I) had the following goals i) to produce a specific map for each direction (Fig. 3), ii) to extract the lineaments of each map and iii) to combine the four results on a global map.

A) N - S							B) E - W						
1	1	1	2	1	1	1	-1	-1	-1	0	1	1	1
1	1	2	3	2	1	1	-1	-1	-2	0	2	3	1
1	2	3	4	3	2	1	-1	-2	-3	0	3	2	1
0	0	0	0	0	0	0	-2	-3	-4	0	4	3	2
-1	-2	-3	-4	-3	-2	-1	-1	-2	-3	0	3	2	1
-1	-1	-2	-3	-2	-1	-1	-1	-1	-2	0	2	3	1
-1	-1	-1	-2	-1	-1	-1	-1	-1	-1	0	1	1	1
D) NE - SW							**C) NW - SE**						
0	1	1	1	1	1	2	2	1	1	1	1	1	0
-1	0	2	2	2	3	1	1	3	2	2	2	0	-1
-1	-2	0	3	4	2	1	1	2	4	3	0	-2	-1
-1	-2	-3	0	3	2	1	1	2	3	0	-3	-2	-1
-1	-2	-4	-3	0	2	1	1	2	0	-3	-4	-2	-1
-1	-3	-2	-2	-2	0	1	1	0	-2	-2	-2	-3	-1
-2	-1	-1	-1	-1	-1	0	0	-1	-1	-1	-1	-1	-2

Table II.- Sobel filters in four principal directions.

Tabla II.- Filtros sobel en cuatro direcciones principales.

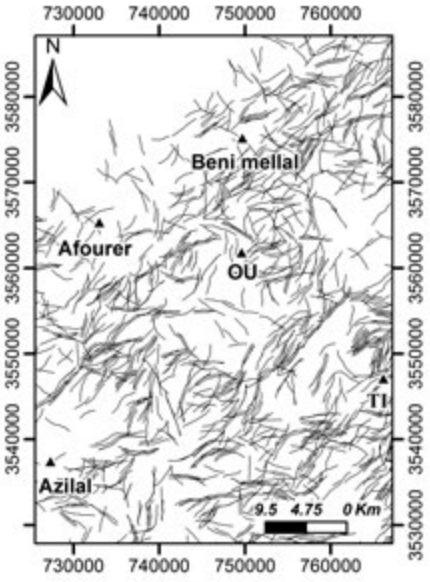

Fig. 3.- Automatic lineaments map.

Fig. 3.- Mapa automático de líneas.

On the other hand, considering the pixel size of 30x30 m, the 7x7 sobel filter will only consider contrasts with a thickness greater than or equal to 210 m. Therefore, we will avoid any anthropogenic or artificial source lineament.

Sobel's directional filtering allowed us to highlight all lineaments of different sizes and directions.

Results and discussion

The automatic extraction of lineaments gave 1420 lines, with lengths between 0.9 and 11.922 km. The total cumulative length is 9533.44 km. A selection based on the length of the lineaments allowed us to eliminate all segments whose lengths are less than 2 km, in order to target the larger structures such as anticline axes and kilometric scale faults (Fig. 3).

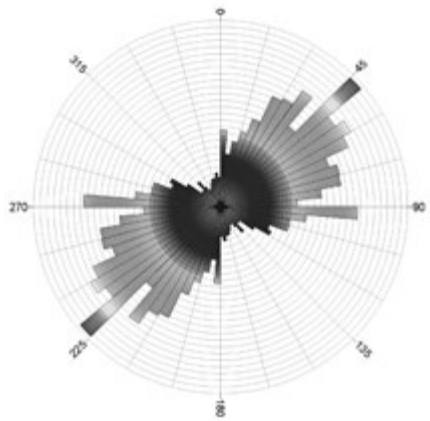

Fig. 4.- Rose diagram of automatic lineaments.

Fig. 4.- Diagrama de rosas de lineamientos automáticos.

Most lineaments show more than one direction. Therefore, variable direction lineaments were divided to obtain the direction of each rectilinear segment. This produced an automatic lineament map with 5527 straight segments or structures. The classification of these segments, based on their lengths, shows a dominance of two classes (2-3 km and 3-4 km), which represent 79.28%. The other classes (5, 6, 7, 8, 9, 10, 11 and 12 km) are less frequent as the longest lineaments are generally rare.

To obtain an idea about the distribution of linear structures extracted automatically, a rose diagram with all directions was produced (Fig. 4).

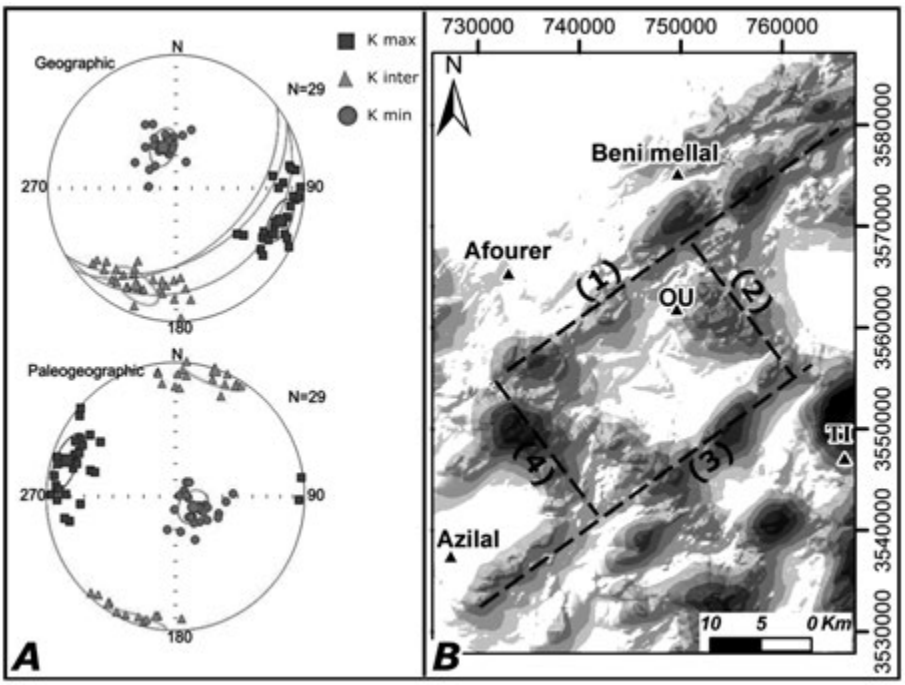

Fig. 5.- A) Magnetic lineations (K_{max} in this figure) before and after bedding correction analysed in Bathonian red beds (Moussaid *et al.*, 2013). B) Lineament density map: (1) Aghbala afourer fault; (2) Tansrift ridge; (3) Abbadine ridge; (4) Ridge R. See color figure in the web.

Fig. 5.- A) Lineación magnética (K_{max} en esta figura) antes y después de la corrección a la horizontal analizada en capas rojas batonienses (Moussaid* et al.*, 2013). B) mapa de densidad de lineamientos: (1) falla de Aghbala-Afourer; (2) cresta de Tansrift; (3) cresta de Abbadine; (4) cresta R. Ver figura en color en la web.

The rose diagram (Fig. 4) evidences the predominance of a NE-SW trend with two relative maxima oriented N0 and N90. Generally, the fracturing density is higher in the competent formations, such as limestone and sandstone, in comparison with soft formations such as clays. On limestone outcrops, the spatial distribution of fracturing is not uniform, with the higher lineament densities following the main structures, showing a striking geometric shape (Fig. 5).

The lineament density map (Fig. 5) highlights higher density of lineaments located around the Ouaouizaght syncline, and coinciding with i) the Jbel Abbadine anticline, which bypasses the Ouaouizaght syncline from the SE with an extension to the SW; ii) the Tansrift ridge separating the Ouaouizaght syncline from that of Taguelft to the eastand iii) the Aghbala-Afourer faulting zone. An additional concentration of lineaments is observed along a NW-SE trending area, separating Ouaouizaght from Aït Attab to the west.

This distribution of fractures defines a rhomboid shape giving a pull apart map view of the Ouaouizaght syncline. This kind of structures is widely observed in the field at small scale, in Jurassic limestones of the the Central High Atlas northern border. This the distribution of fault zones around the Ouaouizaght syncline and the WNW-trending magnetic lineation (obtained from Bathonian series; (Moussaid *et al.*, 2013) are oblique. We interpret this disposition as resulting from stretching of this area under a strike-slip component, dominant in the activation of the Abbadine fault in the south and the major Aghbala-Afourer fault in the north.

As mentioned above, the map of figure 5 shows a higher density of lineaments along four linear zones surrounding the Ouaouizaght syncline. These zones show

different geological features. i) Two of these zones (Jbel Abbadine and Tansrift ridge) show outcrops of Triassic diapiric material, Jurassic gabbroic rocks and unconformities. These structures indicate the synsedimentary activity of these two ridges developed along two major faults controlling sedimentation during the Mesozoic in the Ouaouizaght basin. ii) The Aghbala-Afourer fault is considered as a major paleo-geographic lineament controlling the sedimentation in this area from Jurassic to Mio-Pliocene time (Laville, 1978). iii) The NNW-SSE segment located between Ouaouizaght and Aït Attab synclines does not show any synsedimentary structures in the field or diapiric evidence.

The concentration of brittle structures along the major faults; which coincide with the current anticlines cores of Jbel Abbadine in the south, the Tansrift ridge to east and the Aghbala-Afourer fault in the northern boundary; can lead to explain the high density of lineaments along the western part separating Ouaouizaght from Aït Attab as linked to a synsedimentary ridge developed on a deep basinal fault. The presence of a NW-SE trending syn-sedimentary ridge (ridge "R", 4 in the map of figure 5, between Aït Attab and Ouaouizaght), is consistent with the presence of similar structures (non-diapiric ridges in outcrops) evidenced in the axial part of the central High Atlas using paleomagnetic data (Torres-López *et al.*, 2018).

The frame of synsedimentary ridges around the Ouaouizaght syncline, during the basinal stage, reveals its behavior as a confined area more or less separated from surrounding areas. This gives for the northern boundary of the Central High Atlas an aspect of NE-SW *en-échelon* mini-basins. These mini-basins were inverted to a range of syncline during Cenozoic inversion. Field markers encountered in the western and southern ridges, such as unconformities, changes in lithologies and paleocurrent directions near the basin borders and the presence of conglomeratic levels in some localities neighboring these structures, attest their synsedimentary development and that the Ouaouizaght mini-basin was separated at least from those of Taguelft (east) and Tilouguit (south) and probably from Aït Attab (to the west), during the extensional stage.

Conclusion

The technique of automatic extraction of lineaments has yielded specific results that match with geological field data. This shows the effectiveness of the used method.

The maximum of lineament orientation in the study area shows a NE-SW direction and two relative maxima oriented N0 and N90, which mimic the orientation of structures derived from the extensional Mesozoic and Cenozoic stage. The higher density areas of lineaments are located along the four borders of the Ouaouizaght syncline, probably highlighting the importance of diapiric processes (*e.g.*, movement of salt towards the anticline cores delimiting the Ouaouizaght syncline) during the extensional stage and the relevance of these previous discontinuities in the subsequent tectonic inversion. Almost all of the extracted lineaments are concentrated in the ridge areas surrounding the Ouaouizaght syncline. The directional analysis reveals the dominance of three directions: N0, N90 and N45, conferring a rhomboidal appearance to the synclines of the northern edge of the Central High Atlas.

Acknowledgement

Authors would like to thank Ruth Soto, an anonymous reviewer and Manuel Diaz Azpiroz for their suggestions and comments that helped to improve the manuscript.

References

Haddoumi, Hamid, André Charrière, and Pierre-Olivier Mojon (2010). Geobios 43 (4), 433-451.

Laville E. (1978). *Bulletin de la Société Géologique de France. Fr.* 7, 20, 329-337.

Laville, E. (1985). *Evolution sédimentaire, tectonique et magmatique du Bassin jurassique du Haut Atlas (Maroc): modèle en relais multiples de décrochements.* PhD. Thesis, Univ. Sci. Techn. Languedoc Montepellier, 166 p.

Michard, A., Ibouh, H. and Charrière, A. (2011). *Terra Nova* 23 (5), 314-323.

Monbaron, M. (1985). *Carte géologique du Maroc au 1/100000, feuille de Beni Mellal, Notes et memoires du service géologique du maroc.*

Moore, G.K. and Waltz, F.A. (1983*) Photogrammetric Engineering and Remote Sensing* 49, 641–647.

Moragas Rodriguez, M. (2017). *Multidisciplinary characterization of diapiric basins integrating field examples, numerical and analogue modelling: Central High Atlas Basin (Morocco)* PhD. Thesis, Univ. Barcelona.

Moussaid et al. (2013). *African Earth Sciences* 87 (2013) 13–32.

Nicolini, C. (1980). *Journal of submicroscopic cytology and pathology,* 12(3), 475-505.

O'leary D.W., Freidman J.D. and Pohn H.A. (1976). *Bulletin of the Geological Society of America* 87, 1463–1469.

Saura, E., Verges, J., Martin-Martin, J.D., Messager, G., Moragas, M., Razin, P., Grelaud, C., Joussiaume, R., Malaval, M., Homke, S. and Hunt, D.W. (2014). *Journal of the Geological Society of London* 171, 97–105.

Scanvic, J. Y. (1983). *Utilisation de la télédétection dans les sciences de la terre.* No. 528.8 SCA.

Solomon, S., and Ghebreab, W. (2006). *Journal of African Earth Sciences,* 46(4) 371-378.

Torres-López S., Casas A., Villalaín J.J., Martínez Ruiz V.C., Moussaid B. and El Ouardi H.(2018). *Tectonics*

Van der Werff, H. and van der Meer, F. (2016). *Remote Sensing* 8, 883.